IEM-FT-115/95
hep–ph/9509395

BOUNDS ON THE HIGGS MASS IN THE STANDARD MODEL AND THE MINIMAL SUPERSYMMETRIC STANDARD MODEL [a]

M. QUIROS
CERN, TH Division, CH-1211 Geneva 23, Switzerland
Instituto de Estructura de la Materia, Serrano 123,
28006-Madrid, Spain

Abstract

Depending on the Higgs-boson and top-quark masses, M_H and M_t, the effective potential of the **Standard Model** can develop a non-standard minimum for values of the field much larger than the weak scale. In those cases the standard minimum becomes metastable and the possibility of decay to the non-standard one arises. Comparison of the decay rate to the non-standard minimum at finite (and zero) temperature with the corresponding expansion rate of the Universe allows to identify the region, in the (M_H, M_t) plane, where the Higgs field is sitting at the standard electroweak minimum. In the **Minimal Supersymmetric Standard Model**, approximate analytical expressions for the Higgs mass spectrum and couplings are worked out, providing an excellent approximation to the numerical results which include all next-to-leading-log corrections. An appropriate treatment of squark decoupling allows to consider large values of the stop and/or sbottom mixing parameters and thus fix a reliable upper bound on the mass of the lightest CP-even Higgs boson mass. The discovery of the Higgs boson at LEP 2 might put an upper bound (below the Planck scale) on the scale of new physics Λ and eventually disentangle between the Standard Model and the Minimal Supersymmetric Standard Model.

IEM-FT-115/95
September 1995

[a] Based on talk given at the *International Workshop On Elementary Particle Physics: Present and Future*, Valencia, June 5 to 9, 1995.

1 Lower bounds on the Standard Model Higgs mass

For particular values of the Higgs boson and top quark masses, M_H and M_t, the effective potential of the Standard Model (SM) develops a deep non-standard minimum for values of the field $\phi \gg G_F^{-1/2}$ [1]. In that case the standard electroweak (EW) minimum becomes metastable and might decay into the non-standard one. This means that the SM might not accomodate certain regions of the plane (M_H,M_t), a fact which can be intrinsically interesting as evidence for new physics. Of course, the mere existence of the non-standard minimum, and also the decay rate of the standard one into it, depends on the scale Λ up to which we believe the SM results. In fact, one can identify Λ with the scale of new physics.

1.1 When the EW minimum becomes metastable?

The preliminary question one should ask is: When the standard EW minimum becomes metastable, due to the appearance of a deep non-standard minimum? This question was addressed in past years [1] taking into account leading-log (LL) and part of next-to-leading-log (NTLL) corrections. More recently, calculations have incorporated all NTLL corrections [2,3] resummed to all-loop by the renormalization group equations (RGE), and considered pole masses for the top-quark and the Higgs-boson. From the requirement of a stable (not metastable) standard EW minimum we obtain a lower bound on the Higgs mass, as a function of the top mass, labelled by the values of the SM cutoff (stability bounds). Our result [3] is lower than previous estimates by $\mathcal{O}(10)$ GeV.

The one-loop effective potential of the SM improved by two-loop RGE has been shown to be highly scale independent [4] and, therefore, very reliable for the present study. In Fig. 1 we show (thick solid line) the shape of the effective potential for $M_t = 175$ GeV and $M_H = 121.7$ GeV. We see the appearance of the non-standard maximum, ϕ_M, while the global non-standard minimum has been cutoff at M_P. We can see from Fig. 1 the steep descent from the non-standard maximum. Hence, even if the non-standard minimum is beyond the SM cutoff, the standard minimum becomes metastable and can be destabilized. So for fixed values of M_H and M_t the condition for the standard minimum not to become metastable is

$$\phi_M \gtrsim \Lambda \tag{1}$$

Condition (1) makes the stability condition Λ-dependent. In fact we have plotted in Fig. 2 the stability condition on M_H versus M_t for $\Lambda = 10^{19}$ GeV and 10 TeV. The stability region corresponds to the region above the dashed curves.

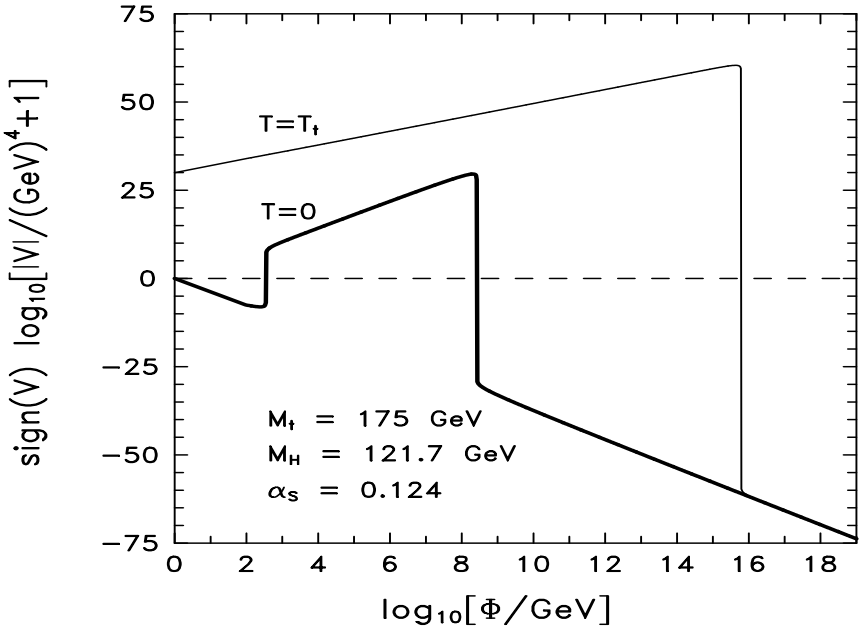

Figure 1: Plot of the effective potential for $M_t = 175$ GeV, $M_H = 121.7$ GeV at $T = 0$ (thick solid line) and $T = T_t = 2.5 \times 10^{15}$ GeV (thin solid line).

1.2 When the EW minimum decays?

In the last subsection we have seen that in the region of Fig. 2 below the dashed line the standard EW minimum is metastable. However we should not draw physical consequences from this fact since we still do not know at which minimum does the Higgs field sit. Thus, the real physical constraint we have to impose is avoiding the Higgs field sitting at its non-standard minimum. In fact the Higgs field can be sitting at its non-standard minimum at zero temperature because:

1. The Higgs field was driven from the origin to the non-standard minimum at finite temperature by thermal fluctuations in a non-standard EW phase transition at high temperature. This minimum evolves naturally to the non-standard minimum at zero temperature. In this case the standard EW phase transition, at $T \sim 10^2$ GeV, will not take place.

2. The Higgs field was driven from the origin to the standard minimum

at $T \sim 10^2$ GeV, but decays, at zero temperature, to the non-standard minimum by a quantum fluctuation.

In Fig. 1 we have depicted the effective potential at $T = 2.5 \times 10^{15}$ GeV (thin solid line) which is the corresponding transition temperature. Our finite temperature potential [5] incorporates plasma effects [6] by one-loop resummation of Debye masses [7]. The tunnelling probability per unit time per unit volume was computed long ago for thermal [8] and quantum [9] fluctuations. At finite temperature it is given by $\Gamma/\nu \sim T^4 \exp(-S_3/T)$, where S_3 is the euclidean action evaluated at the bounce solution $\phi_B(0)$. The semiclassical picture is that unstable bubbles are nucleated behind the barrier at $\phi_B(0)$ with a probability given by Γ/ν. Whether or not they fill the Universe depends on the relation between the probability rate and the expansion rate of the Universe. By normalizing the former with respect to the latter we obtain a normalized probability P, and the condition for decay corresponds to $P \sim 1$. Of course our results are trustable, and the decay actually happens, only if $\phi_B(0) < \Lambda$, so that the similar condition to (1) is

$$\Lambda < \phi_B(0) \tag{2}$$

The condition of no-decay (metastability condition) has been plotted in Fig. 2 (solid lines) for $\Lambda = 10^{19}$ GeV and 10 TeV. The region between the dashed and the solid line corresponds to a situation where the non-standard minimum exists but there is no decay to it at finite temperature. In the region below the solid lines the Higgs field is sitting already at the non-standard minimum at $T \sim 10^2$ GeV, and the standard EW phase transition does not happen.

We also have evaluated the tunnelling probability at zero temperature from the standard EW minimum to the non-standard one. The result of the calculation should translate, as in the previous case, in lower bounds on the Higgs mass for differentes values of Λ. The corresponding bounds are shown in Fig. 2 in dotted lines. Since the dotted lines lie always below the solid ones, the possibility of quantum tunnelling at zero temperature does not impose any extra constraint.

As a consequence of all improvements in the calculation, our bounds are lower than previous estimates [10]. To fix ideas, for $M_t = 175$ GeV, the bound reduces by ~ 10 GeV for $\Lambda = 10^4$ GeV, and ~ 30 GeV for $\Lambda = 10^{19}$ GeV.

2 Upper bounds on the Minimal Supersymmetrics Standard Model lightest Higgs boson mass

The **effective potential** methods to compute the (radiatively corrected) Higgs mass spectrum in the Minimal Supersymmetric Standard Model (MSSM) are

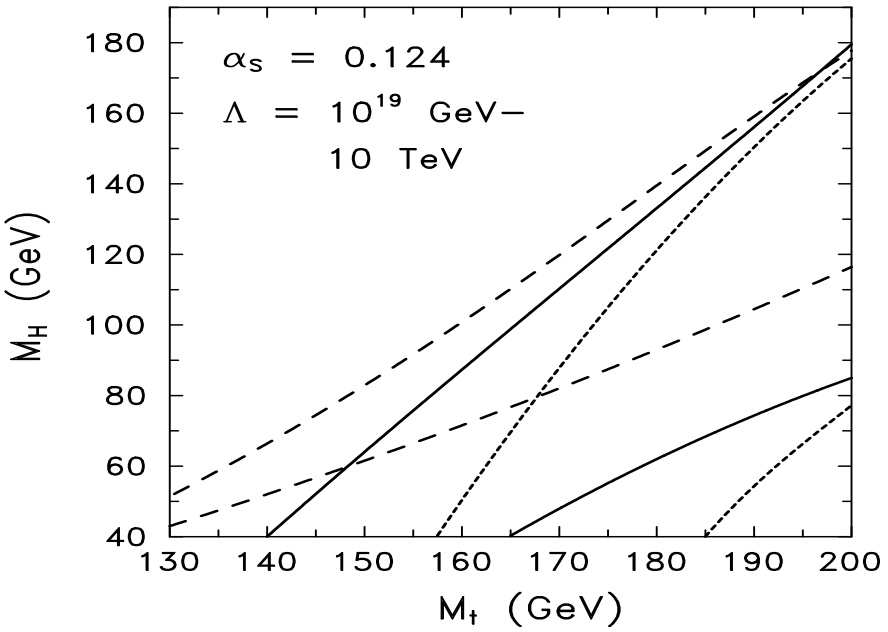

Figure 2: Lower bounds on M_H as a function of M_t, for $\Lambda = 10^{19}$ GeV (upper set) and $\Lambda = 10$ TeV (lower set). The dashed curves correspond to the stability bounds of subsection 1.1 and the solid (dotted) ones to the metastability bounds of subsection 1.2 at finite (zero) temperature.

useful since they allow to **resum** (using Renormalization Group (RG) techniques) LL, NTLL,..., corrections to **all orders** in perturbation theory. These methods [11,12], as well as the diagrammatic methods [13] to compute the Higgs mass spectrum in the MSSM, were first developed in the early nineties.

Effective potential methods are based on the **run-and-match** procedure by which all dimensionful and dimensionless couplings are running with the RG scale, for scales greater than the masses involved in the theory. When the RG scale equals a particular mass threshold, heavy fields decouple, eventually leaving threshold effects in order to match the effective theory below and above the mass threshold. For instance, assuming a common soft supersymmetry breaking mass for left-handed and right-handed stops and sbottoms, $M_S \sim m_Q \sim m_U \sim m_D$, and assuming for the top-quark mass, m_t, and for the CP-odd Higgs mass, m_A, the range $m_t \leq m_A \leq M_S$, we have: for scales $Q \geq M_S$, the MSSM, for $m_A \leq Q \leq M_S$ the two-Higgs doublet model (2HDM), and for

$m_t \leq Q \leq m_A$ the SM. Of course there are thresholds effects at $Q = M_S$ to match the MSSM with the 2HDM, and at $Q = m_A$ to match the 2HDM with the SM.

The neutral Higgs sector of the MSSM contains, on top of the CP-odd Higgs A, two CP-even Higgs mass eigenstates, H_h (the heaviest one) and H (the lightest one). It turns out that the larger m_A the heavier the lightest Higgs H. Therefore the case $m_A \sim M_S$ is, not only a great simplification since the effective theory below M_S is the SM, but also of great interest, since it provides the upper bound on the mass of the lightest Higgs (which is interesting for phenomenological purposes, e.g. at LEP 2). In this case the threshold correction at M_S for the SM quartic coupling λ is:

$$\Delta_{\rm th}\lambda = \frac{3}{16\pi^2} h_t^4 \frac{X_t^2}{M_S^2}\left(2 - \frac{1}{6}\frac{X_t^2}{M_S^2}\right) \tag{3}$$

where h_t is the SM top Yukawa coupling and $X_t = (A_t - \mu/\tan\beta)$ is the mixing in the stop mass matrix, the parameters A_t and μ being the trilinear soft-breaking coupling in the stop sector and the supersymmetric Higgs mixing mass, respectively. The maximum of (3) corresponds to $X_t^2 = 6M_S^2$ which provides the maximum value of the lightest Higgs mass: this case will be referred to as the case of maximal mixing.

We have plotted in Fig. 3 the lightest Higgs pole mass M_H, where all NTLL corrections are resummed to all-loop by the RG, as a function of M_t [4]. From Fig. 3 we can see that the present experimental band from CDF/D0 for the top-quark mass requires $M_H \lesssim 140$ GeV, while if we fix $M_t = 170$ GeV, the upper bound $M_H \lesssim 125$ GeV follows. It goes without saying that these figures are extremely relevant for MSSM Higgs searches at LEP 2.

2.1 An analytical approximation

We have seen [4] that, since radiative corrections are minimized for scales $Q \sim m_t$, when the LL RG improved Higgs mass expressions are evaluated at the top-quark mass scale, they reproduce the NTLL value with a high level of accuracy, for any value of $\tan\beta$ and the stop mixing parameters [14]

$$m_{H,LL}(Q^2 \sim m_t^2) \sim m_{H,NTLL}. \tag{4}$$

Based on the above observation, we can work out a very accurate analytical approximation to $m_{H,NTLL}$ by just keeping two-loop LL corrections at $Q^2 = m_t^2$, i.e. corrections of order t^2, where $t = \log(M_S^2/m_t^2)$.

Again the case $m_A \sim M_S$ is the simplest, and very illustrative, one. We have found [14,15] that, in the absence of mixing (the case $X_t = 0$) two-loop

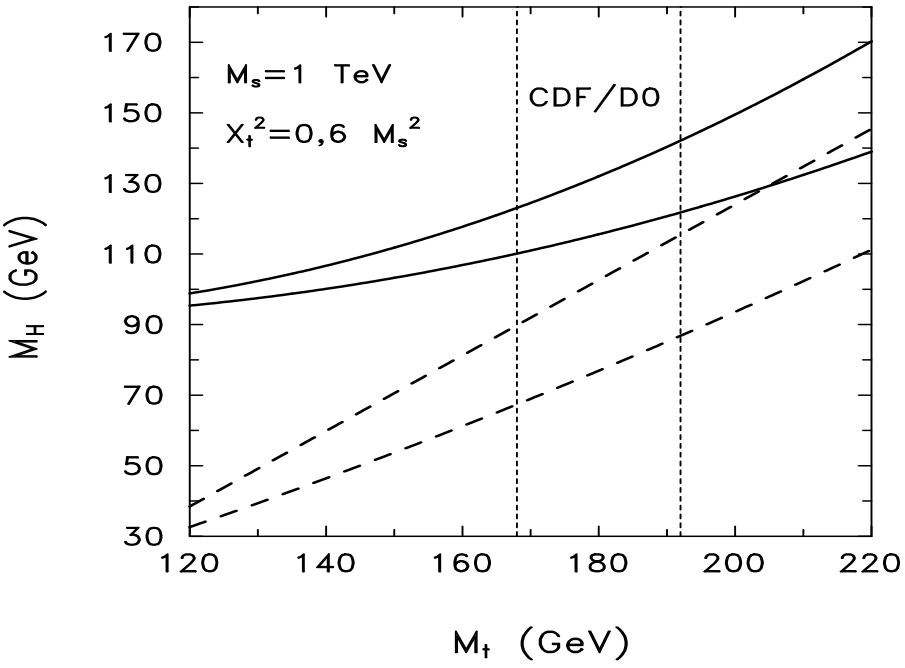

Figure 3: Plot of M_H as a function of M_t for $\tan\beta \gg 1$ (solid lines), $\tan\beta = 1$ (dashed lines), and $X_t^2 = 6M_S^2$ (upper set), $X_t = 0$ (lower set). The experimental band from the CDF/D0 detection is also indicated.

corrections resum in the one-loop result shifting the energy scale from M_S (the tree-level scale) to $\sqrt{M_S\, m_t}$. More explicitly,

$$m_H^2 = M_Z^2 \cos^2 2\beta \left(1 - \frac{3}{8\pi^2} h_t^2\, t\right) + \frac{3}{2\pi^2 v^2} m_t^4(\sqrt{M_S m_t})t \tag{5}$$

where $v = 246.22$ GeV.

In the presence of mixing ($X_t \neq 0$), the run-and-match procedure yields an extra piece in the SM effective potential $\Delta V_{\rm th}[\phi(M_S)]$ whose second derivative gives an extra contribution to the Higgs mass, as

$$\Delta_{\rm th} m_H^2 = \frac{\partial^2}{\partial\phi^2(t)} \Delta V_{\rm th}[\phi(M_S)] = \frac{1}{\xi^2(t)} \frac{\partial^2}{\partial\phi^2(t)} \Delta V_{\rm th}[\phi(M_S)] \tag{6}$$

which, in our case, reduces to

$$\Delta_{\rm th} m_H^2 = \frac{3}{4\pi^2} \frac{m_t^4(M_S)}{v^2(m_t)} \frac{X_t^2}{M_S^2} \left(2 - \frac{1}{6}\frac{X_t^2}{M_S^2}\right) \tag{7}$$

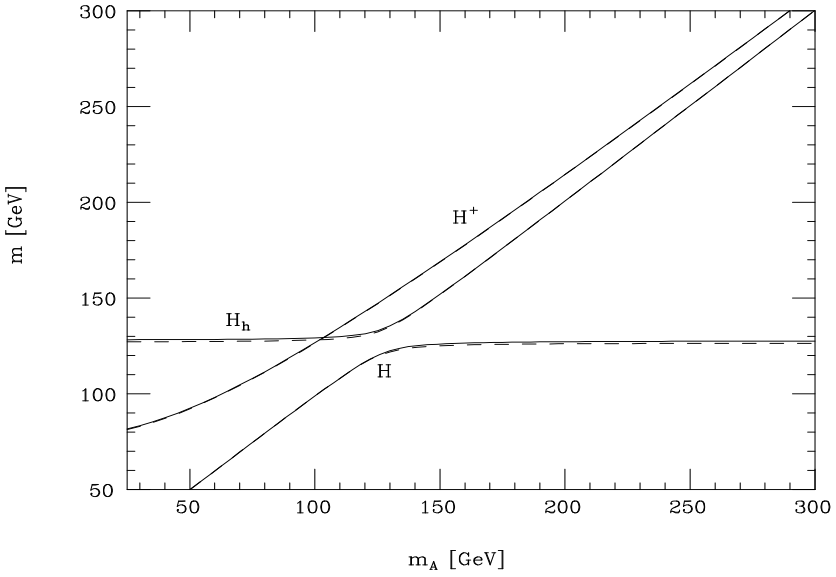

Figure 4: The neutral (H_h, H) and charged (H^+) Higgs mass spectrum as a function of the CP-odd Higgs mass m_A for a physical top-quark mass $M_t = 175$ GeV and $M_S = 1$ TeV, as obtained from the one-loop improved RG evolution (solid lines) and the analytical formulae (dashed lines). All sets of curves correspond to $\tan\beta = 15$ and large squark mixing, $X_t^2 = 6M_S^2$ $(\mu = 0)$.

We have compared our analytical approximation [14] with the numerical NTLL result [4] and found a difference $\lesssim 2$ GeV for all values of supersymmetric parameters.

The case $m_A < M_S$ is a bit more complicated since the effective theory below the supersymmetric scale M_S is the 2HDM. However since radiative corrections in the 2HDM are equally dominated by the top-quark, we can compute analytical expressions based upon the LL approximation at the scale $Q^2 \sim m_t^2$. Our approximation [14] differs from the LL all-loop numerical resummation by $\lesssim 3$ GeV, which we consider the uncertainty inherent in the theoretical calculation, provided the mixing is moderate and, in particular, bounded by the

condition,

$$\left|\frac{m^2_{\widetilde{t}_1} - m^2_{\widetilde{t}_2}}{m^2_{\widetilde{t}_1} + m^2_{\widetilde{t}_2}}\right| \lesssim 0.5 \tag{8}$$

where $\widetilde{t}_{1,2}$ are the two stop mass eigenstates. In Fig. 4 the Higgs mass spectrum is plotted versus m_A.

2.2 Threshold effects

There are two possible caveats in the analytical approximation we have just presented: **i)** Our expansion parameter $\log(M_S^2/m_t^2)$ does not behave properly in the supersymmetric limit $M_S \to 0$, where we should recover the tree-level result. **ii)** We have expanded the threshold function $\Delta V_{\rm th}[\phi(M_S)]$ to order X_t^4. In fact keeping the whole threshold function $\Delta V_{\rm th}[\phi(M_S)]$ we would be able to go to larger values of X_t and to evaluate the accuracy of the approximation (3) and (7). Only then we will be able to check the reliability of the maximum value of the lightest Higgs mass (which corresponds to the maximal mixing) as provided in the previous sections. This procedure has been properly followed [14,16] for the most general case $m_Q \neq m_U \neq m_D$. We have proved that keeping the exact threshold function $\Delta V_{\rm th}[\phi(M_S)]$, and properly running its value from the high scale to m_t with the corresponding anomalous dimensions as in (6), produces two effects: **i)** It makes a resummation from M_S^2 to $M_S^2+m_t^2$ and generates as (physical) expansion parameter $\log[(M_S^2+m_t^2)/m_t^2]$. **ii)** It generates a whole threshold function $X_t^{\rm eff}$ such that (7) becomes

$$\Delta_{\rm th} m_H^2 = \frac{3}{4\pi^2}\frac{m_t^4[M_S^2+m_t^2]}{v^2(m_t)} X_t^{\rm eff} \tag{9}$$

and

$$X_t^{\rm eff} = \frac{X_t^2}{M_S^2+m_t^2}\left(2 - \frac{1}{6}\frac{X_t^2}{M_S^2+m_t^2}\right) + \cdots \tag{10}$$

The numerical calculation shows [16] that $X_t^{\rm eff}$ has the maximum very close to $X_t^2 = 6(M_S^2+m_t^2)$, what justifies the reliability of previous upper bounds on the lightest Higgs mass.

3 Would a light Higgs detection imply new physics?

From the previous sections it should be clear by now that the Higgs and top mass measurements could serve to discriminate between the SM and its extensions, and to provide information about the scale of new physics Λ. In Fig. 5

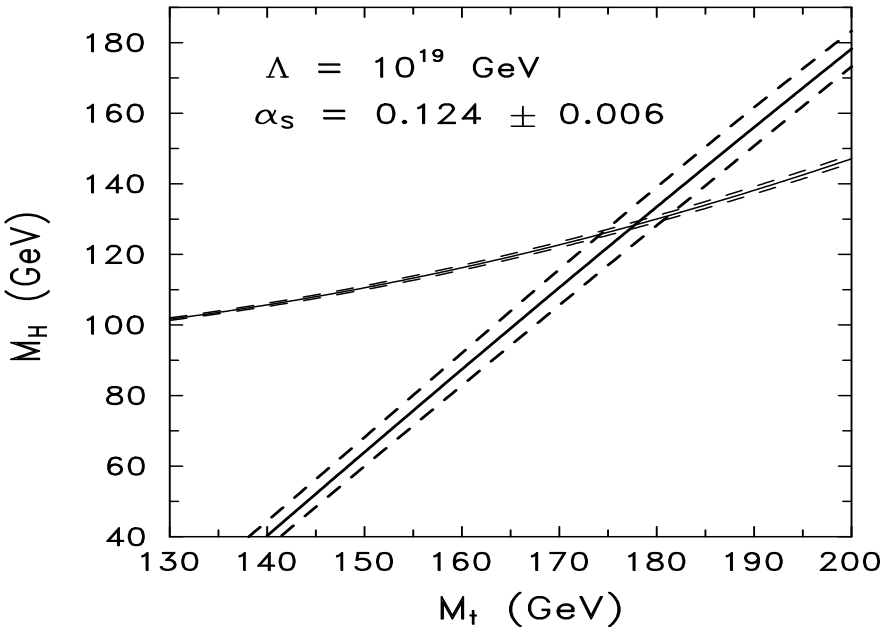

Figure 5: SM lower bounds on M_H (thick lines) as a function of M_t, for $\Lambda = 10^{19}$ GeV, from metastability requirements, and upper bound on the lightest Higgs boson mass in the MSSM (thin lines) for $M_S = 1$ TeV.

we give the SM lower bounds on M_H for $\Lambda \gtrsim 10^{15}$ (thick lines) and the upper bound on the mass of the lightest Higgs boson in the MSSM (thin lines) for $M_S \sim 1$ TeV. Taking, for instance, $M_t = 180$ GeV, which coincides with the central value recently reported by CDF+D0 [17], and $M_H \gtrsim 130$ GeV, the SM is allowed and the MSSM is excluded. On the other hand, if $M_H \lesssim 130$ GeV, then the MSSM is allowed while the SM is excluded. Likewise there are regions where the SM is excluded, others where the MSSM is excluded and others where both are permitted or both are excluded.

Finally from the bounds $M_H(\Lambda)$ (see Fig. 6) one can easily deduce that a measurement of M_H might provide an **upper bound** (below the Planck scale) on the scale of new physics provided that

$$M_t > \frac{M_H}{2.25 \text{ GeV}} + 123 \text{ GeV} \tag{11}$$

Thus, the present experimental bound from LEP, $M_H > 64$ GeV, would imply,

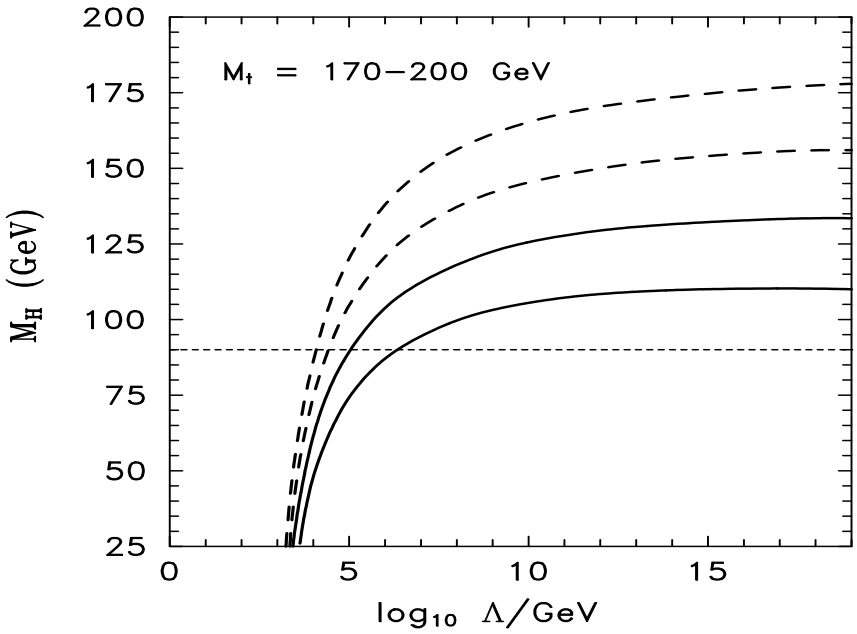

Figure 6: SM lower bounds on M_H from metastability requirements as a function of Λ for different values of M_t.

from (11), $M_t > 152$ GeV, which is fulfilled by experimental detection of the top [17]. Even non-observation of the Higgs at LEP 2 (i.e. $M_H \gtrsim 95$ GeV), would leave an open window ($M_t \gtrsim 163$ GeV) to the possibility that a future Higgs detection at LHC could lead to an upper bound on Λ. Moreover, Higgs detection at LEP 2 would put an upper bound on the scale of new physics. Taking, for instance, $M_H \lesssim 95$ GeV and 170 GeV $< M_t <$ 180 GeV, then $\Lambda \lesssim 10^7$ GeV, while for 180 GeV $< M_t <$ 190 GeV, then $\Lambda \lesssim 10^4$ GeV, as can be deduced from Fig. 6.

Acknowledgments

Work supported in part by the European Union (contract CHRX-CT92-0004) and CICYT of Spain (contract AEN94-0928).

References

1. N. Cabibbo, L. Maiani, G. Parisi and R. Petronzio, *Nucl. Phys.* **B158** (1979) 295; M. Lindner, *Z. Phys.* **C31** (1986) 295; M. Sher, *Phys. Rep.* **179** (1989) 273; M. Lindner, M. Sher and H.W. Zaglauer, *Phys. Lett.* **B228** (1989) 139; M. Sher, *Phys. Lett.* **B317** (1993) 159; Addendum: *Phys. Lett.* **B331** (1994) 448; C. Ford, D.R.T. Jones, P.W. Stephenson and M.B. Einhorn, *Nucl. Phys.* **B395** (1993) 17
2. G. Altarelli and I. Isidori, *Phys. Lett.* **B337** (1994) 141
3. J.A. Casas, J.R. Espinosa and M. Quirós, *Phys. Lett.* **B342** (1995) 171
4. J.A. Casas, J.R. Espinosa, M. Quirós and A. Riotto, *Nucl. Phys.* **B436** (1995) 3; (E) **B439** (1995) 466
5. J.R. Espinosa and M. Quirós, *Phys. Lett.* **B355** (1995) 257
6. For a recent review, see, e.g.: M. Quirós, *Helv. Phys. Acta* **67** (1994) 451
7. L. Dolan and R. Jackiw, *Phys. Rev.* **D9** (1974) 3320; S. Weinberg, *Phys. Rev.* **D9** (1974) 3357; D.J. Gross, R.D. Pisarski and L.G. Yaffe, *Rev. Mod. Phys.* **53** (1981) 43; M.E. Carrington, *Phys. Rev.* **D45** (1992) 2933; M.E. Shaposhnikov, *Phys. Lett.* **B277** (1992) 324 and (E) *Phys. Lett.* **B282** (1992) 483; M. Dine, R.G. Leigh, P. Huet, A. Linde and D. Linde, *Phys. Lett.* **B283** (1992) 319 and *Phys. Rev.* **D46** (1992) 550; J.R. Espinosa and M. Quirós, *Phys. Lett.* **B305** (1993) 98; J.R. Espinosa, M. Quirós and F. Zwirner, *Phys. Lett.* **B314** (1993) 206; C.G. Boyd, D.E. Brahm and S.D. Hsu, *Phys. Rev.* **D48** (1993) 4963; P. Arnold and O. Espinosa, *Phys. Rev.* **D47** (1993) 3546; W. Buchmüller, T. Helbig and D. Walliser, *Nucl. Phys.* **B407** (1993) 387
8. A.D. Linde, *Phys. Lett.* **B70** (1977) 306; *Phys. Lett.* **B100** (1981) 37; *Nucl. Phys.* **B216** (1983) 421
9. S. Coleman, *Phys. Rev.* **D15** (1977) 2929
10. P. Arnold and S. Vokos, *Phys. Rev.* **D44** (1991) 3620
11. Y. Okada, M. Yamaguchi and T. Yanagida, *Prog. Theor. Phys.* **85** (1991) 1; *Phys. Lett.* **B262** (1991) 54; J. Ellis, G. Ridolfi and F. Zwirner, *Phys. Lett.* **B257** (1991) 83; *Phys. Lett.* **B262** (1991) 477; R. Barbieri and M. Frigeni, *Phys. Lett.* **B258** (1991) 395; R. Barbieri, M. Frigeni and F. Caravaglios, *Phys. Lett.* **B258** (1991) 167
12. J.R. Espinosa and M. Quirós, *Phys. Lett.* **B266** (1991) 389
13. H.E. Haber and R. Hempfling, *Phys. Rev. Lett.* **66** (1991) 1815; A. Yamada, *Phys. Lett.* **B263** (1991) 233
14. M. Carena, J.R. Espinosa, M. Quirós and C.E.M. Wagner, *Phys. Lett.* **B355** (1995) 209
15. H.E. Haber, R. Hempfling and A.H. Hoang, CERN preprint, in preparation
16. M. Carena, M. Quirós and C.E.M. Wagner, preprint CERN-TH/95-157

17. F. Abe et al., CDF Collaboration, *Phys. Rev.* **D50** (1994) 2966; *Phys. Rev. Lett.* **73** (1994) 225; preprint FERMILAB-PUB-95/022-E (2 March 1995); S. Abachi et al., D0 Collaboration, *Phys. Rev. Lett.* **72** (1994) 2138; *Phys. Rev. Lett.* **74** (1995) 2422; preprint FERMILAB-PUB-95/028-E (3 March 1995)